

Joint Spectrum and Power Efficiencies Optimization for Statistical QoS Provisionings Over SISO/MIMO Wireless Networks

Wenchi Cheng, Xi Zhang, *Senior Member, IEEE*, and Hailin Zhang, *Member, IEEE*

Abstract—Spectrum and power efficiencies are both crucial to design efficient wireless networks. In past two decades, spectrum and power efficiencies of wireless networks are optimized separately. However, to increase the spectrum efficiency while reducing the energy consumption, it is necessary to jointly optimize spectrum and power efficiencies of wireless networks. Supporting the statistical quality of service (QoS) provisionings for real-time traffic is crucial, but imposes new challenges, in the next generation wireless networks. In this paper, we propose an efficient framework to jointly optimize effective spectrum efficiency (ESE) and effective power efficiency (EPE) under different statistical QoS guarantees constraints to support the real-time traffic over wireless networks. In particular, we derive the relationship between ESE and EPE under statistical QoS provisioning constraint. Based on this relationship, we obtain the mutually beneficial (MB) region and the contention-based (CB) region. In the MB region, we propose a novel strategy to achieve the joint effective spectrum and power efficiencies optimization using the average transmit power control. In the CB region, we propose the wireless-relay-based strategy to jointly optimize the effective capacity and power efficiency. In both MB and CB regions, we develop the dynamic transmit-power control strategy and the MIMO-based strategy to jointly maximize the effective spectrum and power efficiencies. Also conducted is a set of numerical evaluations showing that our proposed strategies can achieve superior joint spectrum and power efficiencies optimization for the diverse statistical QoS provisionings.

Index Terms—Effective capacity, effective spectrum efficiency, effective power efficiency, joint optimization, statistical QoS provisionings, MIMO.

I. INTRODUCTION

ACADEMIA and industry have made tremendous efforts and progresses to improve spectrum efficiency (SE) of wireless networks over the past two decades. A great deal of wireless communication technologies can be employed to increase the SE of wireless networks, such as relay [1], [2],

Manuscript received April 15, 2012; revised November 2, 2012. This work was supported in part by the U.S. National Science Foundation under Grant CNS-205726, the U.S. National Science Foundation CAREER Award under Grant ECCS-0348694, National Natural Science Foundation of China (No.61072069), 111 Project in Xidian University of China (B08038), and Important National Science and Technology Specific Projects (2011ZX0300300104, 2012ZX03003012).

X. Zhang is with the Networking and Information Systems Laboratory, Department of Electrical and Computer Engineering, Texas A&M University, College Station, TX 77843, USA (e-mail: xizhang@ece.tamu.edu) (the corresponding author).

W. Cheng and H. Zhang are with the State Key Laboratory of Integrated Services Networks, Xidian University, Xi'an, 710071, China (e-mails: chengwenchi1986@gmail.com; hlzhang@xidian.edu.cn).

Digital Object Identifier 10.1109/JSAC.2013.130509.

MIMO [3], [4], and cognitive radio [5], [6], etc. On the other hand, due to increasingly demanding of energy cost, which causes large expenditure and CO₂ emission, much research attention has been paid to energy efficiency (EE) or power efficiency (PE) [7]. A wide range of EE and PE optimization schemes have been developed to implement green wireless communications and wireless networks in recent years [8]–[10].

The existing spectrum efficiency optimization schemes aim at maximizing system throughput under specific energy or power constraints [11], [12] while the operative energy or power efficiency optimization schemes seek the minimal system energy consumption under given system throughput requirement [13], [14]. To implement efficient wireless networks, jointly maximizing the spectrum and power efficiencies is more desirable than optimizing SE or PE separately. However, to the best of our knowledge, there is no existing research results where spectrum and power efficiencies are jointly optimized at the same time. Thus, it is crucial to find the effective way to jointly optimize spectrum and power efficiencies for rapid development of wireless networks.

While targeting at jointly optimizing spectrum and power efficiencies, we also need to take into consideration the quality of service (QoS) provisionings for real-time multimedia traffics over wireless networks. Due to the time-varying channels, deterministic QoS to support real-time applications is not possible in realistic wireless networks. Consequently, the statistical QoS guarantee, in terms of QoS exponent and effective capacity has become an important alternative to support real-time wireless transmissions in wireless networks [15]–[17]. To efficiently optimize spectrum and power efficiencies jointly, we also need to take the statistical QoS guarantees into account.

Recently, there are a large number of studies looking at achieving energy efficient picocells/femtocells as described in [18], [19]. These works mainly focus on developing efficient strategies to switch picocells/femtocells into sleeping mode as many as possible while guaranteeing the QoS requirements for mobile cellular users. However, putting some picocells/femtocells into sleeping mode will inevitably cause some coverage holes that are originally covered by some sleeping picocells/femtocells. In addition, these works on picocells/femtocells do not take into account the delay-QoS requirements. Also, there are some works concentrating on exploiting power efficient Coordinated Multiple-Points (CoMP)

transmission/reception to reduce the energy consumption of wireless networks as described in [20], [21]. However, these works also do not take the delay-QoS requirements into consideration either.

To overcome the aforementioned problems, in this paper we propose an efficient framework to jointly optimize effective spectrum efficiency (ESE) and effective power efficiency (EPE) under different statistical QoS provisionings constraints. We derive the relationship between the ESE and the EPE under various statistical QoS guarantees. In the relationship identified by our framework, we identify two critical operating regions: *mutual beneficial (MB) region* and *contention-based (CB) region* to determine whether the ESE and the EPE can be jointly optimized or not using the average transmit power control. In the MB region, the ESE and the EPE both increase as the average transmit power increases. While in the CB region, the ESE increases and the EPE decreases as the average transmit power increases. We analyze the global maximum EPE and the global optimal average transmit power under different statistical QoS guarantees. In the MB region, we develop a new strategy to implement joint effective spectrum and power efficiencies optimization using the average transmit power control. In the CB region, we propose the wireless-relay-based strategy to achieve the joint effective capacity and power efficiency optimization. In both MB and CB regions, we develop the dynamic transmit power control strategy and the multiple-input-multiple-output (MIMO)-based strategy to jointly optimize the ESE and the EPE.

The rest of this paper is organized as follows. Section II describes the system model and defines the ESE and the EPE. Section III derives the relationship between the ESE and the EPE under various statistical QoS guarantees. Based on the relationship, we analyze the impact of statistical QoS guarantees on the global maximum EPE and the global optimal average transmit power. Section IV develops a new strategy to jointly optimize effective spectrum and power efficiencies using the average transmit power control in the MB region. We also propose the wireless-relay-based strategy to achieve the effective capacity and power efficiency optimization in the CB region. Section V develops the dynamic transmit power control strategy and the MIMO-based strategy to jointly optimize the ESE and the EPE, respectively, in both MB and CB regions. Section VI conducts numerical analyses to evaluate our joint spectrum and power efficiencies optimization. The paper concludes with Section VII.

II. THE SYSTEM MODEL

Consider a point-to-point link between the transmitter and the receiver over single-input-single-output (SISO)/MIMO wireless networks as shown in Fig. 1. A first-in-first-out (FIFO) queue buffer is implemented at the transmitter, which is comprised of the upper-layer packets to be transmitted to the receiver. These packets are divided into frames at the link-layer and then split into bit-streams at the physical-layer. Based on the QoS constraint θ (to be detailed soon in Section II-A) required by the service, the transmitter needs to determine the optimal transmit power to jointly optimize the effective spectrum and power efficiencies. We concentrate on discrete-time channel, indexed by $i = 1, 2, \dots$, with stationary and

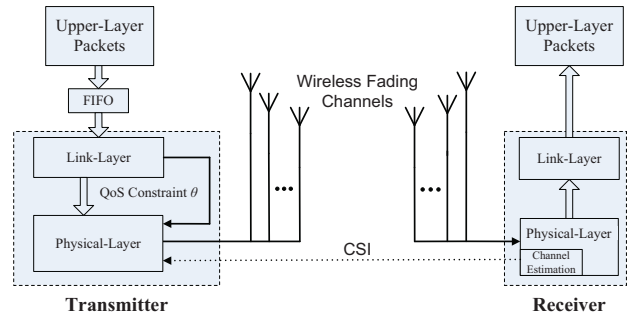


Fig. 1. The point-to-point link under statistical QoS guarantees over SISO/MIMO wireless networks.

ergodic time-varying gain $\sqrt{g[i]}$, $0 \leq g[i]$, and additive white Gaussian noise (AWGN) $n[i]$. The channel power gain $g[i]$ follows a given distribution $d(g)$, for example, for Rayleigh fading, $d(g)$ is an exponential distribution. The channel power gain $g[i]$ varies as time index i changes. In this paper, we consider the block fading channel, where $g[i]$ is constant during the i -th time frame, but changes to another value at the $(i+1)$ -th time frame based on the distribution $d(g)$. Let $\bar{P}_t(\theta)$ denote the average transmit signal power, $N_0/2$ represent the noise power spectral density of $n[i]$, and B denote the received signal bandwidth. The instantaneous received signal-to-noise ratio (SNR), also called the channel state information (CSI), is then given by $\gamma[i] = \bar{P}_t(\theta)g[i]/(N_0B)$. Since $\bar{P}_t(\theta)/(N_0B)$ is a constant, the distribution of $g[i]$ determines the distribution of $\gamma[i]$. By estimating the CSI at the receiver and feeding back the CSI to the transmitter through the feedback channel, the distribution of $\gamma[i]$ can be known to both the transmitter and receiver. However, due to the delay of the feedback channel, the transmitter is not guaranteed to be able to timely receive $\gamma[i]$ at time i at the transmitter. Therefore, in terms of the knowledge of $\gamma[i]$ at the transmitter at time i , we need to consider two different scenarios: (1) The value of $g[i]$ is known at the receiver, but not known at the transmitter, at time i ; (2) The value of $\gamma[i]$ is known at both the transmitter and receiver at time i for the case where the feedback channel delay is small and neglectable [12]. For scenario (1), only the average transmit power control strategy can be applied at the transmitter. For scenario (2), both the average and dynamic transmit power control strategies can be implemented at the transmitter.

We use the Rayleigh channel model in our wireless system, which is one of the most commonly used models to characterize wireless fading channels. The probability density function (PDF) of Rayleigh channel, denoted by $p_{\mathcal{R}}(\gamma[i])$, can be written as $p_{\mathcal{R}}(\gamma[i]) = (e^{-\gamma[i]/\bar{\gamma}})/\bar{\gamma}$, where $\bar{\gamma}$ is the average SNR of the wireless channel.

A. The Spectrum Efficiency for Statistical QoS Guarantees

Based on large deviation principle, the author of [22] showed that under sufficient conditions, the queue length process $Q(t)$ converges in distribution to a random variable $Q(\infty)$ such that

$$-\lim_{Q_{th} \rightarrow \infty} \frac{\log(\Pr\{Q(\infty) > Q_{th}\})}{Q_{th}} = \theta \quad (1)$$

where Q_{th} is the queue length bound and the parameter $\theta > 0$ is a real-valued number. The parameter θ , which is called the *QoS exponent*, indicates the exponential decay rate of the delay-bound QoS violation probabilities. A larger θ corresponds to a faster decay rate, which implies that the system can provide a more *stringent* QoS requirement. A smaller θ leads to a slower decay rate, which implies a *looser* QoS requirement. Asymptotically, when $\theta \rightarrow \infty$, this implies that the system cannot tolerate any delay, which corresponds to the very stringent QoS constraint. On the other hand, when $\theta \rightarrow 0$, the system can tolerate an arbitrarily long delay, which corresponds to the very loose QoS constraint.

Let the sequence $\{R[i], i = 1, 2, \dots\}$ denote a discrete-time stationary and ergodic stochastic service process and $S[t] = \sum_{i=1}^t R[i]$ represents the partial sum of the service process over time sequence of $i = 1, 2, \dots, t$. The Gärtner – Ellis limit of $S[t]$, expressed as $\Lambda_C(\theta) = \lim_{t \rightarrow \infty} (1/t) \log (\mathbb{E} \{e^{\theta S[t]}\})$, is a convex function differentiable for all real-valued θ , where $\mathbb{E}\{\cdot\}$ denotes the expectation. Inspired by the principle of effective bandwidth [23], the authors in [15] defined effective capacity as the maximum constant arrival rate which can be supported by the service rate to guarantee the specified QoS exponent θ . If the service-rate sequence $R[i]$ is stationary and time uncorrelated, the effective capacity can be written as [17]

$$\mathcal{C}(\theta) = -\frac{1}{\theta} \log \left(\mathbb{E} \left\{ e^{-\theta R[i]} \right\} \right). \quad (2)$$

Consequently, we can define the effective spectrum efficiency (ESE), denoted by $\mathcal{C}_q(\theta, \bar{P}_t(\theta))$, as follows:

$$\begin{aligned} \mathcal{C}_I(\theta) &= -\frac{1}{\theta} \log \left(\mathbb{E} \left\{ e^{-\theta \tilde{R}[i]} \right\} \right) \\ &= -\frac{1}{\theta} \log \left(\mathbb{E}_\gamma \left\{ e^{-\theta \log_2(1+P_t(\theta, \gamma))} \right\} \right), \end{aligned} \quad (3)$$

where $\mathbb{E}_\gamma\{\cdot\}$ is the expectation over γ , $P_t(\theta, \gamma)$ denotes the instantaneous transmit power corresponding to the CSI γ and the required QoS exponent θ , and $\tilde{R}[i] = \log_2(1 + P_t(\theta, \gamma))$ represents the service-rate per Hz per second. On the right-hand of the second equality of Eq. (3) and in the following discussions, we omit the time-index i for simplicity. Since the dynamic transmit power control can only be implemented when the transmitter can get the instantaneous CSI, the ESE $\mathcal{C}_I(\theta)$ given in Eq. (3) cannot be achieved when the transmitter cannot get the instantaneous CSI. Therefore, in the case where the transmitter only knows the distribution of the CSI and cannot get the instantaneous CSI γ , we further define the ESE, denoted by $\mathcal{C}_q(\theta, \bar{P}_t(\theta))$, as follows:

$$\mathcal{C}_q(\theta, \bar{P}_t(\theta)) = -\frac{1}{\theta} \log \left(\mathbb{E}_\gamma \left\{ e^{-\theta \log_2(1+\bar{P}_t(\theta)\gamma)} \right\} \right), \quad (4)$$

where $\bar{P}_t(\theta) = \mathbb{E}_\gamma\{P_t(\theta, \gamma)\}$ is the average transmit power. From Eqs. (3) and (4), we can see that $\mathcal{C}_q(\theta, \bar{P}_t(\theta))$ is a tight lower-bound of $\mathcal{C}_I(\theta)$ [17].

B. The Power Efficiency for Statistical QoS Guarantees

We model the power consumption for statistical QoS guarantees, denoted by $P_o(\theta)$, as follows:

$$P_o(\theta) = \alpha \mathbb{E}_\gamma \{P_t(\theta, \gamma)\} + P_c = \alpha \bar{P}_t(\theta) + P_c, \quad (5)$$

where α is the average-transmit power-consumption coefficient that scales up with the average transmit power due to amplifier loss. Thus, intuitively, $\alpha \in [1, \infty)$ is the reciprocal of the power amplifier efficiency which varies in the range of $(0, 1]$. The term P_c is the circuit power consumption which is independent of the average transmit power. For both mobile devices (for example, smart phones and tablets) and picocell/femtocell access points, P_c corresponds to signal processing, transmitter idling, and transmitter power conservation.

Our proposed power consumption model is appropriate, adequate to, and well fits our queuing model. When the queue is empty, the transmitter remains idle corresponding to $\bar{P}_t(\theta) = 0$ and the circuit power consumption stays the same as in the case that the queue is not empty. To maintain the operation of the transmitter, the circuit power still needs to be consumed even when the queue is empty. Therefore, it is rational to consider the power consumption in our queuing model. Only if the transmitter can accurately predict the time when the new data comes and leaves, the transmitter can avoid the circuit power consumption when the queue is empty. Then, to further reduce the energy consumption when the queue is empty, we can employ one of the popular device-sleeping strategies which have been discussed by a number of recent works as described in [24], [25]. However, this is not the focus of this paper and thus its discussions are beyond the scope of this paper.

To evaluate the power efficiency under statistical QoS guarantees, we define the effective power efficiency (EPE), denoted by $\mathcal{E}_q(\theta, \bar{P}_t(\theta))$, as follows:

$$\begin{aligned} \mathcal{E}_q(\theta, \bar{P}_t(\theta)) &= \frac{\mathcal{C}_q(\theta, \bar{P}_t(\theta))}{P_o(\theta)} \\ &= \frac{-\frac{1}{\theta} \log \left(\mathbb{E}_\gamma \left\{ e^{-\theta \log_2(1+\bar{P}_t(\theta)\gamma)} \right\} \right)}{\alpha \bar{P}_t(\theta) + P_c}. \end{aligned} \quad (6)$$

Clearly, $\mathcal{C}_q(\theta, \bar{P}_t(\theta))$ and $P_o(\theta)$ both monotonically increase as the average transmit power $\bar{P}_t(\theta)$ increases.

Our proposed QoS-guaranteed power consumption model can be efficiently applied to the devices that the circuit power consumption P_c does not overwhelm the total power consumption $P_o(\theta)$ such as smart phones, tablets, WiFi access points, picocell access points, and femtocell access points. However, for the devices that the circuit power consumption P_c overwhelms the total power consumption $P_o(\theta)$ (for example, the base stations), it is more straightforward and effective to just use those popular device-sleeping strategies as proposed in [24], [25].

Our purpose is to jointly optimize the effective spectrum and power efficiencies. In the following, we derive the relationship between the ESE and the EPE. Then, we analyze the impact of statistical QoS guarantees on joint effective spectrum and power efficiencies optimization. Based on these analyses, we propose strategies to jointly optimize the effective spectrum and power efficiencies in the mutual beneficial or/and contention-based regions (to be detailed in Section III-A).

III. SPECTRUM EFFICIENCY AND POWER EFFICIENCY FOR SISO WIRELESS NETWORKS

From Eq. (4), we see that the ESE increases as the average transmit power increases. From Eq. (6), we can obtain the relationship between the EPE and the average transmit power. Thus, we can derive the relationship between the ESE and the EPE through the average transmit power.

A. The Mutual Beneficial Region and Contention-Based Region Under Various Delay-QoS Guarantees

Theorem 1: If the requested QoS exponent is equal to θ , then for the given the feasible ESE region $[\mathcal{C}_q^{\text{REQ}}(\theta), \infty)$, the ESE, denoted by $\mathcal{C}_q^*(\theta)$, which maximizes the EPE $\mathcal{E}_q(\theta, \bar{P}_t(\theta))$ given by Eq. (6), is determined by

$$\mathcal{C}_q^*(\theta) = \begin{cases} \mathcal{C}_q^{\text{REQ}}(\theta), & \mathcal{C}_q^{\text{REQ}}(\theta) > \mathcal{C}_q(\theta, P_q^E(\theta)) \\ \mathcal{C}_q(\theta, P_q^E(\theta)), & \mathcal{C}_q^{\text{REQ}}(\theta) \leq \mathcal{C}_q(\theta, P_q^E(\theta)) \end{cases} \quad (7)$$

where $\mathcal{C}_q^{\text{REQ}}(\theta) \in [0, \infty)$ is the lower-bound of feasible region of the ESE and $P_q^E(\theta)$ is the global optimal average transmit power corresponding to the feasible ESE region $[0, \infty)$. The global optimal average transmit power $P_q^E(\theta)$ can be numerically obtained through the following equation:

$$P_q^E(\theta) = \frac{\mathcal{C}_q(\theta, P_q^E(\theta))}{\left. \frac{\partial \mathcal{C}_q(\theta, \bar{P}_t(\theta))}{\partial \bar{P}_t(\theta)} \right|_{\bar{P}_t(\theta)=P_q^E(\theta)}} - \frac{P_c}{\alpha}. \quad (8)$$

Proof: For a requested θ , taking the derivative of $\mathcal{C}_q(\theta, \bar{P}_t(\theta))$ given in Eq. (4) with respect to $\bar{P}_t(\theta)$, we can get:

$$\frac{\partial \mathcal{C}_q(\theta, \bar{P}_t(\theta))}{\partial \bar{P}_t(\theta)} = \mathbb{E}_\gamma \left\{ \frac{\gamma e^{-\theta \log_2(1+\bar{P}_t(\theta)\gamma)}}{\mathbb{E}_\gamma \left\{ e^{-\theta \log_2(1+\bar{P}_t(\theta)\gamma)} \right\} (1 + \bar{P}_t(\theta)\gamma) \log 2} \right\} > 0, \quad (9)$$

which is larger than zero because all terms in Eq. (9) are larger than zero. The derivative of $\mathcal{E}_q(\theta, \bar{P}_t(\theta))$ with respect to $\bar{P}_t(\theta)$ can be derived as follows:

$$\frac{\partial \mathcal{E}_q(\theta, \bar{P}_t(\theta))}{\partial \bar{P}_t(\theta)} = \frac{\frac{\partial \mathcal{C}_q(\theta, \bar{P}_t(\theta))}{\partial \bar{P}_t(\theta)} (\alpha \bar{P}_t(\theta) + P_c) - \mathcal{C}_q(\theta, \bar{P}_t(\theta)) \alpha}{(\alpha \bar{P}_t(\theta) + P_c)^2}. \quad (10)$$

From Eqs. (9)-(10), we can obtain the derivative of $\mathcal{E}_q(\theta, \bar{P}_t(\theta))$ with respect to $\mathcal{C}_q(\theta, \bar{P}_t(\theta))$ as follows:

$$\frac{\partial \mathcal{E}_q(\theta, \bar{P}_t(\theta))}{\partial \mathcal{C}_q(\theta, \bar{P}_t(\theta))} = \frac{\frac{\partial \mathcal{E}_q(\theta, \bar{P}_t(\theta))}{\partial \bar{P}_t(\theta)}}{\frac{\partial \mathcal{C}_q(\theta, \bar{P}_t(\theta))}{\partial \bar{P}_t(\theta)}} = \frac{\frac{\partial \mathcal{C}_q(\theta, \bar{P}_t(\theta))}{\partial \bar{P}_t(\theta)} (\alpha \bar{P}_t(\theta) + P_c) - \mathcal{C}_q(\theta, \bar{P}_t(\theta)) \alpha}{\frac{\partial \mathcal{C}_q(\theta, \bar{P}_t(\theta))}{\partial \bar{P}_t(\theta)} (\alpha \bar{P}_t(\theta) + P_c)^2}. \quad (11)$$

Define a new function $G(\theta, \bar{P}_t(\theta))$ to represent the nominator expression in the most right-hand-side part of Eq. (11) as follows:

$$G(\theta, \bar{P}_t(\theta)) \triangleq \frac{\partial \mathcal{C}_q(\theta, \bar{P}_t(\theta))}{\partial \bar{P}_t(\theta)} (\alpha \bar{P}_t(\theta) + P_c) - \mathcal{C}_q(\theta, \bar{P}_t(\theta)) \alpha. \quad (12)$$

Because $\partial \mathcal{C}_q(\theta, \bar{P}_t(\theta)) / \partial \bar{P}_t(\theta)$ (which is larger than 0 as shown in the derivation of Eq. (9)) and $(\alpha \bar{P}_t(\theta) + P_c)^2$ are both larger than zero, judging the sign of Eq. (11) can be determined by just evaluating the sign of Eq. (12). Taking derivative of $G(\theta, \bar{P}_t(\theta))$ with respect to $\bar{P}_t(\theta)$, we can obtain:

$$\frac{\partial G(\theta, \bar{P}_t(\theta))}{\partial \bar{P}_t(\theta)} = \frac{\partial^2 \mathcal{C}_q(\theta, \bar{P}_t(\theta))}{\partial (\bar{P}_t(\theta))^2} (\alpha \bar{P}_t(\theta) + P_c). \quad (13)$$

Since $(\alpha \bar{P}_t(\theta) + P_c)$ is larger than zero, judging the sign of $[\partial G(\theta, \bar{P}_t(\theta)) / \partial (\bar{P}_t(\theta))] / \partial \bar{P}_t(\theta)$ is equivalent to judging the sign of $[\partial^2 \mathcal{C}_q(\theta, \bar{P}_t(\theta)) / \partial (\bar{P}_t(\theta))^2]$. On the other hand, because of Eq. (4) and the fact that $[\log(\mathbb{E}_\gamma\{\mu\}) / \theta]$ is linear with respect to μ , we can observe that judging the sign of $[\partial^2 \mathcal{C}_q(\theta, \bar{P}_t(\theta)) / \partial (\bar{P}_t(\theta))^2]$ is equivalent to judging the sign of $[-\partial^2(e^{-\theta \log_2(1+\bar{P}_t(\theta)\gamma)}) / \partial (\bar{P}_t(\theta))^2]$. Then, we can derive and obtain the following equations:

$$-\frac{\partial^2 \left(e^{-\theta \log_2(1+\bar{P}_t(\theta)\gamma)} \right)}{\partial (\bar{P}_t(\theta))^2} = -\frac{\theta \gamma^2}{\log 2} \left(\frac{\theta}{\log 2} + 1 \right) (1 + \bar{P}_t(\theta)\gamma)^{-\frac{\theta}{\log 2} - 2} < 0, \quad (14)$$

which implies $[\partial^2 \mathcal{C}_q(\theta, \bar{P}_t(\theta)) / \partial (\bar{P}_t(\theta))^2]$ is less than zero. Due to $(\alpha \bar{P}_t(\theta) + P_c) > 0$, we have $[\partial G(\theta, \bar{P}_t(\theta)) / \partial \bar{P}_t(\theta)] < 0$. Thus, $G(\theta, \bar{P}_t(\theta))$ monotonically decreases as $\bar{P}_t(\theta)$ increases. Set $G(\theta, \bar{P}_t(\theta)) \big|_{\bar{P}_t(\theta)=P_q^E(\theta)} = 0$ in Eq. (12), we can obtain Eq. (8). Then, $G(\theta, \bar{P}_t(\theta))$ is larger/less than zero when $\bar{P}_t(\theta)$ is less/larger than $P_q^E(\theta)$. Therefore, $\mathcal{E}_q(\theta, \bar{P}_t(\theta))$ monotonically increases/decreases as $\mathcal{C}_q(\theta, \bar{P}_t(\theta))$ increases when $\bar{P}_t(\theta)$ is less/larger than $P_q^E(\theta)$. Thus, Eq. (7) follows. ■

To better understand the insights given by Theorem 1, we plot the curves of the EPE versus the ESE under different statistical QoS guarantees $\theta = 0.1, 1, \text{ and } 10$, respectively, in Fig. 2, where we assume $P_c = 40$ dBm and $\alpha = 1$. Observing Figs. 2(a)-(c), we have the following remark.

Remark 1: The MB region and the CB region are divided by the vertical line where the ESE is equal to $\mathcal{C}_q(\theta, P_q^E(\theta))$ (see vertical dash lines in Fig. 2.). In the MB region, where $\mathcal{C}_q(\theta, \bar{P}_t(\theta)) < \mathcal{C}_q(\theta, P_q^E(\theta))$, the ESE and the EPE both increase as the average transmit power increases. While in the CB region ($\mathcal{C}_q(\theta, \bar{P}_t(\theta)) \geq \mathcal{C}_q(\theta, P_q^E(\theta))$), the ESE increases and the EPE decreases as the average transmit power increases. Therefore, in the MB region, the ESE and the EPE can be jointly optimized through increasing the average transmit power. However, in the CB region, it is impossible to jointly increase the ESE and the EPE by increasing the average transmit power.

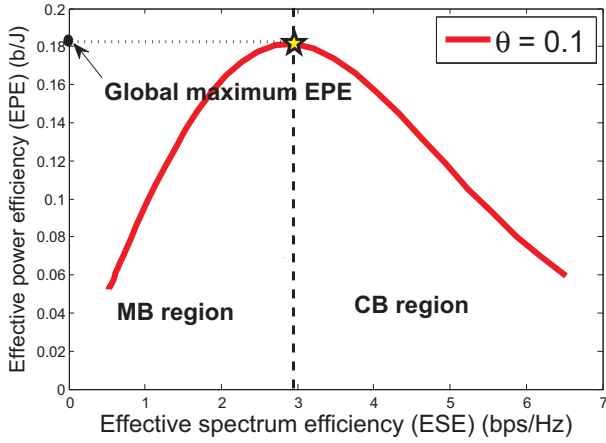
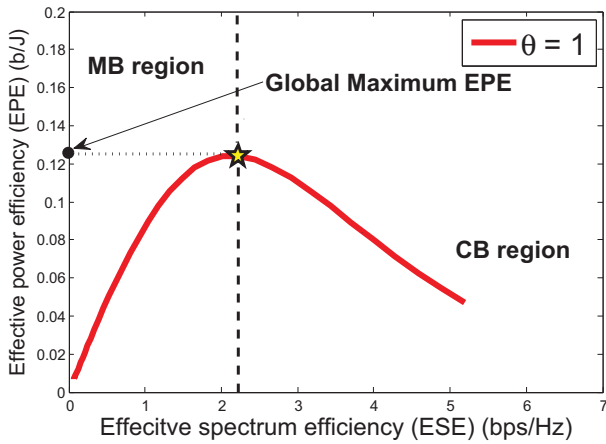
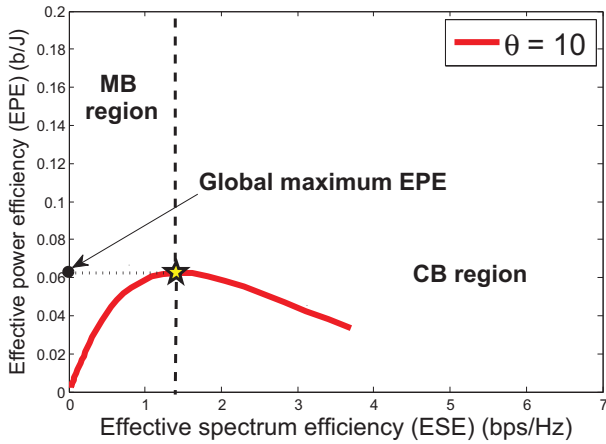

 (a) $\theta = 0.1$.

 (b) $\theta = 1$.

 (c) $\theta = 10$.

Fig. 2. The mutual beneficial and contention-based regions.

B. The Global Optimal Effective Power Efficiency and Average Transmit Power Under Various Delay-QoS Guarantees

We characterize the impact of statistical QoS guarantees on the global maximum power efficiency and the global optimal average transmit power by the following two propositions, where we let θ_1 and θ_2 be two different QoS exponents, assuming $\theta_1 < \theta_2$.

Proposition 1: Given the feasible ESE region $[0, \infty)$, when the effective spectrum efficiencies corresponding to θ_1 and θ_2 are the same, i.e., $C_q(\theta_1, \bar{P}_t(\theta_1)) = C_q(\theta_2, \bar{P}_t(\theta_2))$, where $\bar{P}_t(\theta_1)$ and $\bar{P}_t(\theta_2)$ are the average transmit power corresponding to θ_1 and θ_2 , respectively, the EPE corresponding to θ_1 is larger than the EPE corresponding to θ_2 , i.e., $\mathcal{E}_q(\theta_1, \bar{P}_t(\theta_1)) > \mathcal{E}_q(\theta_2, \bar{P}_t(\theta_2))$.

Proof: When the QoS exponent increases from θ_1 to θ_2 , to guarantee the same ESE $C_q(\theta_1, \bar{P}_t(\theta_1)) = C_q(\theta_2, \bar{P}_t(\theta_2))$, $\bar{P}_t(\theta_2)$ needs to be larger than $\bar{P}_t(\theta_1)$. Thus, we have

$$\frac{C_q(\theta_1, \bar{P}_t(\theta_1))}{\alpha \bar{P}_t(\theta_1) + P_c} > \frac{C_q(\theta_2, \bar{P}_t(\theta_2))}{\alpha \bar{P}_t(\theta_2) + P_c}. \quad (15)$$

Then, from Eq. (6) we can obtain Proposition 1. \blacksquare

Proposition 2: Given the feasible ESE region $[0, \infty)$, the global maximum EPE corresponding to θ_1 is larger than the global maximum EPE corresponding to θ_2 , i.e., $\mathcal{E}_q(\theta_1, P_q^E(\theta_1)) > \mathcal{E}_q(\theta_2, P_q^E(\theta_2))$, where $P_q^E(\theta_1)$ and $P_q^E(\theta_2)$ are the global optimal average transmit power corresponding to θ_1 and θ_2 , respectively.

Proof: From Proposition 1 we can derive $\mathcal{E}_q(\theta_2, P_q^E(\theta_2)) < \mathcal{E}_q(\theta_1, P_1)$, where P_1 can be obtained from $C_q(\theta_1, P_1) = C_q(\theta_2, P_q^E(\theta_2))$. On the other hand, because $\mathcal{E}_q(\theta_1, P_q^E(\theta_1))$ is the maximum of EPE for θ_1 , we have $\mathcal{E}_q(\theta_1, P_1) \leq \mathcal{E}_q(\theta_1, P_q^E(\theta_1))$, where the equality holds only when $P_q^E(\theta_1) = P_1$. Thus, we have $\mathcal{E}_q(\theta_2, P_q^E(\theta_2)) < \mathcal{E}_q(\theta_1, P_q^E(\theta_1))$. \blacksquare

Remark 2: As indicated by Propositions 1 and 2, the global maximum EPE decreases as QoS exponent increases. This is because as the delay-bound QoS becomes stringent, the original global maximum EPE cannot be kept to be a constant through increasing average transmit power.

Then, we can characterize the impact of statistical QoS guarantees on the global optimal average transmit power by Proposition 3, before which we first analyze a useful function by Lemma 1 given as follows.

Lemma 1: The following defined function

$$f(\theta, \bar{P}_t(\theta)) = \frac{e^{-\theta \log_2(1 + \bar{P}_t(\theta)\gamma)}}{\mathbb{E}_\gamma \left\{ e^{-\theta \log_2(1 + \bar{P}_t(\theta)\gamma)} \right\}} \quad (16)$$

monotonically increases as θ increases, where $\theta \in [0, \infty)$.

Proof: Taking the derivative of $f(\theta)$ with respect to θ , we can get

$$\frac{\partial f(\theta, \bar{P}_t(\theta))}{\partial \theta} = \frac{e^{-\theta \log_2(1 + \bar{P}_t(\theta)\gamma)} \log_2(1 + \bar{P}_t(\theta)\gamma)}{\left(\mathbb{E}_\gamma \left\{ e^{-\theta \log_2(1 + \bar{P}_t(\theta)\gamma)} \right\} \right)^2} \cdot \left[\mathbb{E}_\gamma \left\{ e^{-\theta \log_2(1 + \bar{P}_t(\theta)\gamma)} \right\} - e^{-\theta \log_2(1 + \bar{P}_t(\theta)\gamma)} p_\Gamma(\gamma) \right]. \quad (17)$$

Because we have

$$\mathbb{E}_\gamma \left\{ e^{-\theta \log_2(1 + \bar{P}_t(\theta)\gamma)} \right\} > e^{-\theta \log_2(1 + \bar{P}_t(\theta)\gamma)} p_\Gamma(\gamma), \quad (18)$$

we can obtain $\partial f(\theta, \bar{P}_t(\theta)) / \partial \theta > 0$. Thus, Lemma 1 follows. \blacksquare

The proposition given below shows that the global optimal transmit power is a monotonically increasing function of QoS exponent θ .

Proposition 3: The global optimal transmit power corresponding to θ_1 is less than the global optimal transmit power corresponding to θ_2 , i.e., $P_q^E(\theta_1) < P_q^E(\theta_2)$.

Proof: The ESE $C_q(\theta, P_q^E(\theta))$ is a monotonically decreasing function of θ when $P_q^E(\theta)$ remains as a constant. Substituting $\bar{P}_t(\theta) = P_q^E(\theta)$ into Eq. (9), we have

$$\begin{aligned} I(\theta, P_q^E(\theta)) &= \frac{\partial C_q(\theta, \bar{P}_t(\theta))}{\partial \bar{P}_t(\theta)} \Big|_{\bar{P}_t(\theta)=P_q^E(\theta)} \\ &= \mathbb{E}_\gamma \left\{ \frac{\gamma p_\Gamma(\gamma) f(\theta, P_q^E(\theta))}{(1 + P_q^E(\theta)\gamma) \log 2} \right\}. \end{aligned} \quad (19)$$

From Lemma 1 we can obtain that $I(\theta, P_q^E(\theta))$ monotonically increases as θ increases. Then, we study the sign of the parameter K defined as follows:

$$K = \frac{\partial \mathcal{E}_q(\theta_2, \bar{P}_t(\theta_2))}{\partial C_q(\theta_2, \bar{P}_t(\theta_2))} \Big|_{C_q(\theta_2, \bar{P}_t(\theta_2))=C_q(\theta_2, P_q^E(\theta_1))}. \quad (20)$$

Because $C_q(\theta_1, \bar{P}_t(\theta_1))$ and $I(\theta_1, P_q^E(\theta_1))$ decreases and increases as θ_1 increases, respectively, we have

$$\begin{aligned} \frac{C_q(\theta_2, P_q^E(\theta_1))}{I(\theta_2, P_q^E(\theta_1))} - \frac{P_c}{\alpha} &< \frac{C_q(\theta_1, P_q^E(\theta_1))}{I(\theta_1, P_q^E(\theta_1))} - \frac{P_c}{\alpha} \\ &= P_q^E(\theta_1). \end{aligned} \quad (21)$$

From Eqs. (11) and (21), we can obtain $K > 0$. Thus, $(C_q(\theta_2, P_q^E(\theta_1)), \mathcal{E}_q(\theta_2, P_q^E(\theta_1)))$ is in the mutual beneficial region corresponding to θ_2 . Then, we have $P_q^E(\theta_1) < P_q^E(\theta_2)$ and thus, Proposition 3 follows. ■

Remark 3: As indicated by Proposition 3, the global optimal average transmit power increases as QoS exponent increases. However, increasing of the global optimal average transmit power cannot compensate for the decreasing of the EPE due to the increasing of QoS exponent.

IV. TWO DIFFERENT POWER CONTROL STRATEGIES CORRESPONDING TO MUTUAL BENEFICIAL AND CONTENTION-BASED REGIONS

Because the EPE increases as the ESE increases in the MB region, we propose the average power control strategy, named JESPEO strategy, to jointly increase the EPE and the ESE in the MB region. Taking into account the tradeoff between the ESE and the EPE in the CB region, we propose the wireless-relay-based strategy to increase the effective capacity and the EPE.

A. The Average Transmit Power Control in the Mutual Beneficial (MB) Region

Denote the required and the maximum achievable ESEs by $s_r(\theta)$ and $s_a(\theta)$, respectively. Then, we give the criterion for joint effective spectrum and power efficiencies optimization (JESPEO) as follows:¹

JESPEO Criterion:

CASE 1: When $s_r(\theta)$ and $s_a(\theta)$ are both less than $C_q(\theta, P_q^E(\theta))$, it is desirable to use the maximum average

¹For a given QoS exponent θ , we assume the maximum achievable effective spectrum efficiency $s_a(\theta)$ is always not less than the required effective spectrum efficiency $s_r(\theta)$.

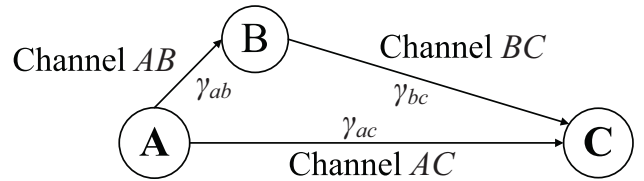


Fig. 3. The wireless relay system.

transmit power to achieve the maximum EPE and the maximum ESE $s_a(\theta)$;

CASE 2: When $s_r(\theta)$ is less than $C_q(\theta, P_q^E(\theta))$ and $s_a(\theta)$ is larger than $C_q(\theta, P_q^E(\theta))$, it is desirable to use the global optimal average transmit power $P_q^E(\theta)$ to achieve the global maximum EPE and the corresponding ESE $C_q(\theta, P_q^E(\theta))$;

CASE 3: When $s_r(\theta)$ is larger than $C_q(\theta, P_q^E(\theta))$, the maximum EPE corresponds to the minimum ESE while the maximum ESE corresponds to the minimum EPE.

Based on the JESPEO criterion described in the above, we can give the corresponding strategy, named *JESPEO strategy*, for the joint effective spectrum and power efficiencies optimization as follows:

- **For CASE 1:** Using the maximum average transmit power corresponding to the maximum achievable ESE $s_a(\theta)$;
- **For CASE 2:** Using the global optimal average transmit power $P_q^E(\theta)$;
- **For CASE 3:** Using the JESPEO criterion, it is impossible to jointly optimize the effective spectrum and the power efficiencies through average transmit power control because the EPE decreases as the ESE increases.

Remark 4: Because in the MB region, the EPE and the ESE both increase as the average transmit power increases, if the required ESE falls into the MB region, we can increase the average transmit power until it reaches to the value of $P_q^E(\theta)$ to achieve the global maximum EPE and increase the ESE at the same time. However, the JESPEO strategy cannot jointly increase the EPE and the ESE in the CB region.

B. Joint Effective Capacity and Effective Power Efficiency Optimization in the Contention-Based (CB) Region

For a wide bandwidth wireless system, the effective capacity is more important than the ESE. Thus, in our wireless system, the joint effective spectrum and power efficiencies optimization needs to be replaced by the joint effective capacity and effective power efficiency optimization.

We consider a typical wireless relay system as shown in Fig. 3. The data of node A can be transmitted to node C through the direct channel AC. The node B can receive the data of node A through channel AB and transmit node A's data to node C through the channel BC. The channels AC and AB use the same frequency band. The channels AC and BC are frequency orthogonal. We denote the instantaneous channel SNR as γ_{ac} , γ_{ab} , and γ_{bc} corresponding to the channels AC, AB, and BC, respectively. For simplicity, we assume the bandwidth of the channels AC and BC are both W . The average transmit power of node A and node B are $\bar{P}_a(\theta)$ and

$\bar{P}_b(\theta)$, respectively. The circuit power consumptions of node A and node B are both P_c . Therefore, the effective capacity of our relay wireless system, denoted by $\mathcal{C}_R(\theta)$, can be written as follows:

$$\mathcal{C}_R(\theta) = -\frac{1}{\theta} \log \left(\mathbb{E}_{\gamma_{ac}} \left\{ e^{-\theta \log_2(1 + \bar{P}_a(\theta) \gamma_{ac})} \right\} \right) - \frac{1}{\theta} \log \left(\mathbb{E}_{\gamma_{bc}} \left\{ e^{-\theta \log_2(1 + \bar{P}_b(\theta) \gamma_{bc})} \right\} \right) \quad (22)$$

where W is normalized to be 1 and we assume the channel AB is good enough to decode the node A's data at the node B with insignificant errors. The EPE of our relay wireless system, denoted by $\mathcal{E}_R(\theta)$, can be derived as follows:

$$\mathcal{E}_R(\theta) = \frac{\mathcal{C}_R(\theta)}{\alpha(\bar{P}_a(\theta) + \bar{P}_b(\theta)) + 2P_c}. \quad (23)$$

We denote the required effective capacity by $\mathcal{C}_M(\theta)$. We also represent the minimum required average transmit power and the corresponding EPE when only using the direct channel by $\bar{P}_M(\theta)$ and $\mathcal{E}_M(\theta)$, respectively. The values of $\bar{P}_a(\theta)$ and $\bar{P}_b(\theta)$ can be obtained from the feasibility problem, denoted by **F1**, as follows [26]:

$$\mathbf{F1:} \quad \text{find } \{(\bar{P}_a(\theta), \bar{P}_b(\theta))\} \quad (24)$$

$$\text{s.t. : } 1). \mathcal{C}_R(\theta) = \mathcal{C}_M(\theta); \quad (25)$$

$$2). 0 < \bar{P}_a(\theta) < \bar{P}_M(\theta), 0 < \bar{P}_b(\theta) < \bar{P}_M(\theta). \quad (26)$$

Then, we give the wireless-relay-based strategy as follows:

1). We solve the feasibility problem **F1** to obtain the feasible $\bar{P}_a(\theta)$ and $\bar{P}_b(\theta)$;

2). If $(\mathcal{C}_q(\theta, \bar{P}_a(\theta)), \mathcal{E}_q(\theta, \bar{P}_a(\theta)))$ is in the MB region, we increase $\bar{P}_a(\theta)$ until it reaches the value of $P_q^E(\theta)$;

3). If $(\mathcal{C}_q(\theta, \bar{P}_b(\theta)), \mathcal{E}_q(\theta, \bar{P}_b(\theta)))$ is in the MB region, we increase $\bar{P}_b(\theta)$ until it reaches the value of $P_q^E(\theta)$.

From the constraint given by Eq. (25), we see that the required effective capacity is guaranteed. After solving the feasibility problem **F1**, the node A's data can be transmitted to node C using two orthogonal channels AC and BC with average transmit power $\bar{P}_a(\theta)$ and $\bar{P}_b(\theta)$ at node A and node B, respectively. If $\bar{P}_a(\theta)$ is less than the value of $P_q^E(\theta)$, we increase $\bar{P}_a(\theta)$ until it reaches the value of $P_q^E(\theta)$. If $\bar{P}_b(\theta)$ is less than the value of $P_q^E(\theta)$, we increase $\bar{P}_b(\theta)$ until it reaches the value of $P_q^E(\theta)$. We plot Fig. 4 to illustrate our wireless-relay-based strategy. As shown in Fig. 4, let symbol X denote the point on the curve corresponding to the coordinate $(\mathcal{C}_M(\theta), \mathcal{E}_M(\theta))$, where $\mathcal{C}_M(\theta)$ and $\mathcal{E}_M(\theta)$ are the required effective capacity and the EPE corresponding to $\mathcal{C}_M(\theta)$ when only using the direct channel to transmit node A's data to node C. The pentagram symbol denotes the point with coordinate $(\mathcal{C}_q(\theta, P_q^E(\theta)), \mathcal{E}_q(\theta, P_q^E(\theta)))$. The left-hand and the right-hand of the vertical dash line are the MB region and the CB region, respectively. Then, after solving the feasibility problem **F1**, we can obtain the average transmit power $\bar{P}_a(\theta)$ and $\bar{P}_b(\theta)$ corresponding to the channels AC and BC , respectively. The effective capacity of the channels AC and BC are $\mathcal{C}_q(\theta, \bar{P}_a(\theta))$ and $\mathcal{C}_q(\theta, \bar{P}_b(\theta))$, respectively. We denote four typical points on the curve with symbols X_1, X_2, X_3 , and X_4 , respectively, where X_1 and X_2 are in the MB region while X_3 and X_4 are in the CB region.

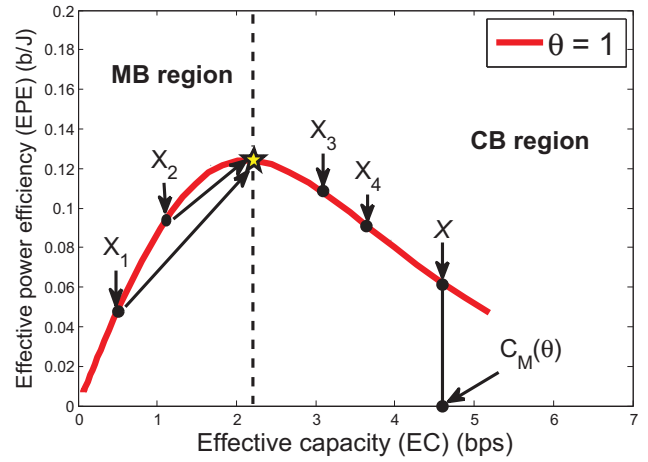


Fig. 4. The wireless-relay-based strategy.

We assume $(\mathcal{C}_q(\theta, \bar{P}_a(\theta)), \mathcal{E}_q(\theta, \bar{P}_a(\theta))) \in \{X_1, X_3\}$ and $(\mathcal{C}_q(\theta, \bar{P}_b(\theta)), \mathcal{E}_q(\theta, \bar{P}_b(\theta))) \in \{X_2, X_4\}$ because both $(\mathcal{C}_q(\theta, \bar{P}_a(\theta)), \mathcal{E}_q(\theta, \bar{P}_a(\theta)))$ and $(\mathcal{C}_q(\theta, \bar{P}_b(\theta)), \mathcal{E}_q(\theta, \bar{P}_b(\theta)))$ will definitely fall into either the MB region or the CB region. If $(\mathcal{C}_q(\theta, \bar{P}_a(\theta)), \mathcal{E}_q(\theta, \bar{P}_a(\theta)))$ falls into the MB region, we increase $\bar{P}_a(\theta)$ until it reaches to $P_q^E(\theta)$. If $(\mathcal{C}_q(\theta, \bar{P}_b(\theta)), \mathcal{E}_q(\theta, \bar{P}_b(\theta)))$ falls into the MB region, we increase $\bar{P}_b(\theta)$ until it reaches to $P_q^E(\theta)$.

Before comparing the values between $\mathcal{E}_R(\theta)$ and $\mathcal{E}_M(\theta)$, we first prove the following analytical result by Fact 1.

Fact 1: For real-valued variables $v_1 > 0$, $v_2 > 0$, $v_3 > 0$, and $v_4 > 0$, if $(v_1/v_2) > \tilde{v}$ and $(v_3/v_4) > \tilde{v}$ exist, we have $[(v_1 + v_3)/(v_2 + v_4)] > \tilde{v}$.

Proof: Because we have $[(v_1 + v_3)/(v_2 + v_4)] > \{[\tilde{v}(v_2 + v_4)]/(v_2 + v_4)\} = \tilde{v}$, Fact 1 follows. ■

Using Fact 1, if the inequality

$$\begin{cases} \frac{-\frac{1}{\theta} \log \left(\mathbb{E}_{\gamma_{ac}} \left\{ e^{-\theta \log_2(1 + \bar{P}_a(\theta) \gamma_{ac})} \right\} \right)}{\alpha \bar{P}_a(\theta) + P_c} > \mathcal{E}_M(\theta) \\ \frac{-\frac{1}{\theta} \log \left(\mathbb{E}_{\gamma_{bc}} \left\{ e^{-\theta \log_2(1 + \bar{P}_b(\theta) \gamma_{bc})} \right\} \right)}{\alpha \bar{P}_b(\theta) + P_c} > \mathcal{E}_M(\theta) \end{cases} \quad (27)$$

holds, we have $\mathcal{E}_R(\theta) > \mathcal{E}_M(\theta)$. Then, we need to consider the following four cases:

- **CASE I:** If $\bar{P}_a(\theta) \geq P_q^E(\theta)$ and $\bar{P}_b(\theta) \geq P_q^E(\theta)$, it is clear that Eq. (27) holds. Thus, we have $\mathcal{E}_R(\theta) > \mathcal{E}_M(\theta)$ and $\mathcal{C}_R(\theta) = \mathcal{C}_M(\theta)$;
- **CASE II:** If $\bar{P}_a(\theta) < P_q^E(\theta)$ and $\bar{P}_b(\theta) \geq P_q^E(\theta)$, we increase $\bar{P}_a(\theta)$ until it reaches the value of $P_q^E(\theta)$. Then, Eq. (27) holds. Thus, we have $\mathcal{E}_R(\theta) > \mathcal{E}_M(\theta)$ and $\mathcal{C}_R(\theta) > \mathcal{C}_M(\theta)$;
- **CASE III:** If $\bar{P}_a(\theta) \geq P_q^E(\theta)$ and $\bar{P}_b(\theta) < P_q^E(\theta)$, we increase $\bar{P}_b(\theta)$ until it reaches the value of $P_q^E(\theta)$. Then, Eq. (27) holds. Thus, we have $\mathcal{E}_R(\theta) > \mathcal{E}_M(\theta)$ and $\mathcal{C}_R(\theta) > \mathcal{C}_M(\theta)$;
- **CASE IV:** If $\bar{P}_a(\theta) < P_q^E(\theta)$ and $\bar{P}_b(\theta) < P_q^E(\theta)$, we both increase $\bar{P}_a(\theta)$ and $\bar{P}_b(\theta)$ until they reach the value of $P_q^E(\theta)$. Then, Eq. (27) holds. Thus, we have $\mathcal{E}_R(\theta) > \mathcal{E}_M(\theta)$ and $\mathcal{C}_R(\theta) > \mathcal{C}_M(\theta)$.

Remark 5: By solving the feasibility problem **F1**, we can obtain the feasible average transmit power $\bar{P}_a(\theta)$ and $\bar{P}_b(\theta)$ for the channels AB and BC , respectively. For CASE I, the achieved EPE increases and the achieved effective capacity is kept to be the same as the required effective capacity. For CASE II, CASE III, and CASE IV, the achieved effective capacity and the achieved EPE both increase as compared with the required effective capacity and the EPE corresponding to the required effective capacity. Our wireless-relay-based strategy allocates the transmit power over the wide bandwidth to increase the EPE and the effective capacity at the same time. Although the new relay resource is introduced, we have taken into account the newly added power consumption imposed by the relay node in our model. In Eq. (23), we take into account the power consumptions of both the source node $[\alpha\bar{P}_a(\theta) + P_c]$ and the relay node $[\alpha\bar{P}_b(\theta) + P_c]$. Therefore, it is fair to compare the effective capacity and the EPE between the case of using wireless-relay-based strategy and the case of using average-transmit power-control strategy for the direct channel. Using the wireless-relay-based strategy, the effective capacity and the EPE can be jointly increased as compared with the case using the average-transmit power-control strategy for the direct channel, as illustrated by CASE I, CASE II, CASE III, and CASE IV, where we show that the effective capacity/EPE of using the wireless-relay-based strategy $\mathcal{C}_R(\theta)/\mathcal{E}_R(\theta)$ is always larger than or equal to the effective capacity/EPE of using the average-transmit power-control strategy for the direct channel $\mathcal{C}_M(\theta)/\mathcal{E}_M(\theta)$ in the CB region. Thus, it is beneficial to use the wireless-relay-based strategy for jointly optimizing the effective capacity and the EPE in the CB region.

V. TWO DIFFERENT POWER CONTROL SCHEMES FOR JOINT EFFECTIVE SPECTRUM AND POWER EFFICIENCIES OPTIMIZATION IN BOTH MUTUAL BENEFICIAL AND CONTENTION-BASED REGIONS

In this section, we propose another two power control strategies to jointly optimize effective spectrum and power efficiencies in *both* MB and CB regions. In the first power control strategy, the transmitter uses the instantaneous CSI received from the receiver to dynamically allocate transmit power over time. We name this strategy as the dynamic transmit power control strategy. The second power control strategy is based on the multiple-input-multiple-output (MIMO) multiplexing technique. Thus, we can call this strategy as MIMO-based strategy.

A. The Dynamic Transmit Power Control Strategy for Joint Effective Spectrum and Power Efficiencies Optimization

If the transmitter can receive the instantaneous CSI timely, we can use the dynamic transmit power control to jointly optimize the effective spectrum and power efficiencies. When we apply the dynamic transmit power control, we need to rewrite the EPE, denoted by $\mathcal{E}_I(\theta)$, as follows:

$$\begin{aligned} \mathcal{E}_I(\theta) &= \frac{\mathcal{C}_I(\theta)}{\alpha \mathbb{E}_\gamma \{P_t(\theta, \gamma)\} + P_c} \\ &= \frac{-\frac{1}{\theta} \log \left(\mathbb{E}_\gamma \left\{ e^{-\theta \log_2(1+P_t(\theta, \gamma))} \right\} \right)}{\alpha \bar{P}_t(\theta) + P_c}. \end{aligned} \quad (28)$$

From Eqs. (3) and (28), we see that when the average transmit power $\bar{P}_t(\theta)$ is fixed for a given QoS exponent θ , the increasing of $\mathcal{C}_I(\theta)$ through the dynamic transmit power control can increase $\mathcal{E}_I(\theta)$ at the same time. Thus, joint effective spectrum and power efficiencies optimization can be achieved by maximizing ESE through the dynamic transmit power control. The joint effective spectrum and power efficiencies optimization problem is converted into maximizing the ESE under the given average transmit power constraint. A large number of dynamic transmit power control strategies and policies can be applied to maximize the spectrum efficiency under the given average transmit power constraint, such as water-filling policy, channel conversion power control policy, and QoS driven instantaneous power control policy.

The optimal dynamic transmit power policy under different delay-QoS constraints is the QoS driven instantaneous power control policy, which is given as follows [17]:

$$P_t(\theta, \gamma) = \begin{cases} 0, & \gamma < \gamma_0; \\ \frac{\bar{P}_t(\theta)}{\gamma_0^{\frac{\beta}{\beta+1}} \gamma^{\frac{\beta}{\beta+1}}} - \frac{\bar{P}_t(\theta)}{\gamma}, & \gamma \geq \gamma_0, \end{cases} \quad (29)$$

where γ_0 is the cut-off SNR threshold and can be numerically obtained by

$$\int_{\gamma_0}^{\infty} P_t(\theta, \gamma) p_\Gamma(\gamma) d\gamma = \bar{P}_t(\theta). \quad (30)$$

When the QoS exponent is very small ($\theta \rightarrow 0$), the QoS driven instantaneous transmit power control policy converges to the well-known water-filling policy. When the QoS exponent is very large ($\theta \rightarrow \infty$), the QoS driven instantaneous transmit power control policy turns to the channel inversion power control policy.

Remark 6: Not only in the MB region, but also in the CB region, the dynamic transmit power control strategy can increase both effective spectrum and power efficiencies.

B. MIMO-Based Power Control Policy for Joint Effective Spectrum and Power Efficiencies Optimization

As we know, if using the multiplexing, the MIMO wireless channels can increase the spectrum efficiency as compared with the wireless channel in SISO-based wireless networks [27]. Therefore, when we fix the total average transmit power of the MIMO wireless channels, we can jointly optimize the effective spectrum and power efficiencies by maximizing the ESE.

When the CSI cannot be sent back to the transmitter timely, we can maximize the ESE by allocating the average transmit power across the transmit antennas over MIMO wireless networks. Then, we can obtain the ESE of the MIMO wireless channels with N_t transmit antennas and N_r receive antennas, denoted by $\mathcal{C}_m(\theta)$, as follows:

$$\mathcal{C}_m(\theta) = -\frac{1}{\theta} \log \left(\mathbb{E}_\gamma \left\{ e^{-\theta \sum_{\ell=1}^L \log_2(1+\bar{P}_t(\theta)\gamma_\ell)} \right\} \right) \quad (31)$$

where $L = \min\{N_t, N_r\}$. Then, we can derive the EPE of the

MIMO wireless channels, denoted by $\mathcal{E}_m(\theta)$, as follows:

$$\begin{aligned} \mathcal{E}_m(\theta) &= \frac{\mathcal{C}_m(\theta)}{\alpha \mathbb{E}_\gamma \left\{ \sum_{\ell=1}^L \bar{P}_\ell(\theta) \right\} + P_c} \\ &= \frac{-\frac{1}{\theta} \log \left(\mathbb{E}_\gamma \left\{ e^{-\theta \sum_{\ell=1}^L \log_2(1 + \bar{P}_\ell(\theta) \gamma_\ell)} \right\} \right)}{\alpha \mathbb{E}_\gamma \left\{ \bar{P}_t(\theta) \right\} + P_c} \end{aligned} \quad (32)$$

where $\bar{P}_\ell(\theta)$ is the average transmit power corresponding to the ℓ th singular-value channel [27].

Because the denominator of Eq. (32) remains as a constant when the total average transmit power $\bar{P}_t(\theta)$ is fixed, we can formulate the joint effective spectrum and power efficiencies optimization problem for the MIMO wireless channels, denoted by **P1**, as follows:

$$\mathbf{P1}: \quad \max_{\bar{P}_\ell(\theta), 1 \leq \ell \leq L} \{ \mathcal{C}_m(\theta) \} \quad (33)$$

$$\text{s.t. :} \quad 1). \quad \mathbb{E}_\gamma \left\{ \sum_{\ell=1}^L \bar{P}_\ell(\theta) \right\} = \mathbb{E}_\gamma \{ \bar{P}_t(\theta) \}; \quad (34)$$

$$2). \quad \bar{P}_\ell(\theta) \geq 0, \quad 1 \leq \ell \leq L. \quad (35)$$

Since the function $-\log\{a\}/\theta$ monotonically decreases as a increases, we can convert problem **P1** to problem **P2**, which has the same solution as problem **P1**, as follows:

$$\mathbf{P2}: \quad \min_{\bar{P}_\ell(\theta), 1 \leq \ell \leq L} \left\{ \mathbb{E}_\gamma \left\{ \prod_{\ell=1}^L (1 + \bar{P}_\ell(\theta) \gamma_\ell)^{-\beta} \right\} \right\} \quad (36)$$

subject to the same constraints specified by Eqs. (34)-(35), where $\beta = \theta/(\log 2)$ is defined as the normalized QoS exponent.

Lemma 2: The objective function of **P2** given in Eq. (36) is strictly convex on the space spanned by $(\bar{P}_1(\theta), \dots, \bar{P}_L(\theta))$.

Proof: The detailed proof of Lemma 2 is provided in Appendix A. ■

Using Lemma 2 and the fact that the functions on the left-hand side of all constraints (Eqs. (34)-(35)) are linear over the space spanned by $(\bar{P}_1(\theta), \dots, \bar{P}_L(\theta))$, we can observe that problem **P2** given by Eq. (36) and Eqs. (34)-(35) is a strictly convex optimization problem. Thus, we can use the Lagrangian method and Karush-Kuhn-Tucker (KKT) conditions to solve this convex optimization problem [26]. To resolve the optimization problem **P2**, we define $\lambda \geq 0$ and $\kappa \geq 0$ to be the Lagrangian multipliers associated with Eqs. (34) and (35), respectively. We also denote the optimal values for λ and κ by λ^* and κ^* , respectively. Next, we define the parameter γ_0 as follows:

$$\gamma_0 \triangleq \frac{\beta}{\lambda^* - \kappa^*}, \quad (37)$$

which is the cut-off threshold of SNR. Then, we can resolve the optimization problem **P2** as characterized by Theorem 2 as follows.

Theorem 2: The optimal solution to **P2** given by Eq. (36) and Eqs. (34)-(35) is determined by

$$\bar{P}_\ell^*(\theta) = \mathbb{E}_\gamma \left\{ \gamma_0^{\frac{1}{1+L\beta}} \prod_{\ell=1}^L \gamma_\ell^{-\frac{\beta}{1+L\beta}} - \frac{1}{\gamma_\ell} \right\}, \quad 1 \leq \ell \leq L. \quad (38)$$

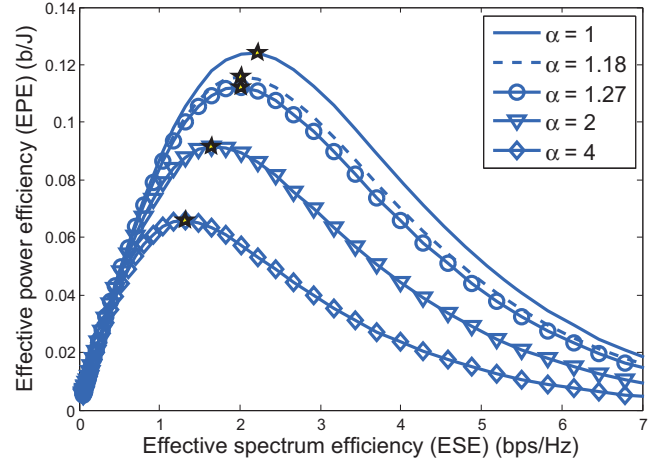


Fig. 5. The impact of the value variation of α on the ESE and the EPE.

where γ_0 given by Eq. (37) can be numerically obtained by substituting Eq. (38) into the following equation:

$$\mathbb{E}_\gamma \left\{ \sum_{\ell=1}^L \bar{P}_\ell^*(\theta) \right\} = \mathbb{E}_\gamma \{ \bar{P}_t(\theta) \}. \quad (39)$$

Proof: The proof of Theorem 2 is provided in Appendix B. ■

Using the average transmit power specified by Theorem 2, we can obtain the maximum ESE for the MIMO wireless channels. Because the total average power of the MIMO wireless channels is fixed, we can also achieve the maximum EPE for the MIMO wireless channels when we maximize the ESE.

Remark 7: The MIMO-based strategy allocates the average transmit power among the transmit antennas to increase the ESE under given total average transmit power constraint, thus increasing the EPE at the same time. As we can observe from Sections V-A and V-B, the dynamic transmit power control strategy and the MIMO-based strategy can be used separated to jointly increase the EPE and the ESE in both MB and CB regions. Furthermore, both of these two strategies can be applied at the same time.

VI. NUMERICAL RESULTS

We use the numerical analyses to evaluate our strategies for joint spectrum and power efficiencies optimization. First, we plot the curves to show the impact of statistical QoS guarantees on the global maximum EPE and the global optimal average transmit power. Second, we evaluate our JESPEO strategy in the MB region. Third, we assess the improvements of both the ESE and the EPE by using the dynamic transmit power control strategy and the MIMO-based strategy, respectively, for both MB and CB regions. In Figs. 6 and 7, P_c is set to be 37 dBm, 40 dBm, and 43 dBm, respectively. In Figs. 8-11, P_c is set to be 40 dBm. In Figs. 6-11, the average SNR of the channel is set to be 0 dB.

Figure 5 shows the impact of the value variation of α on the ESE and the EPE when $\theta = 1$, where we set $\alpha = 1, 1.18, 1.27, 2, \text{ and } 4$, respectively, corresponding to that the amplifier

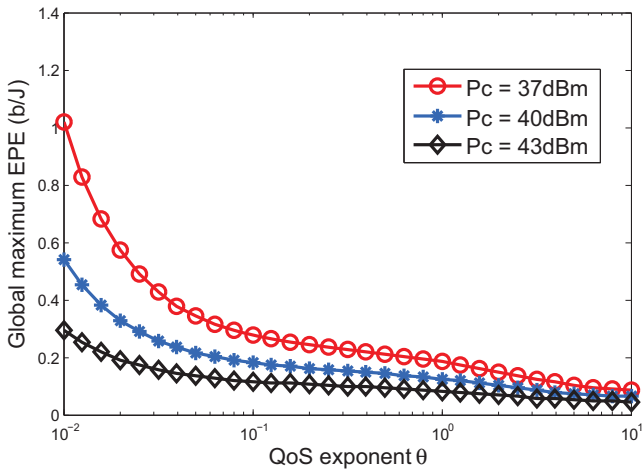


Fig. 6. The global maximum EPE under various QoS exponent.

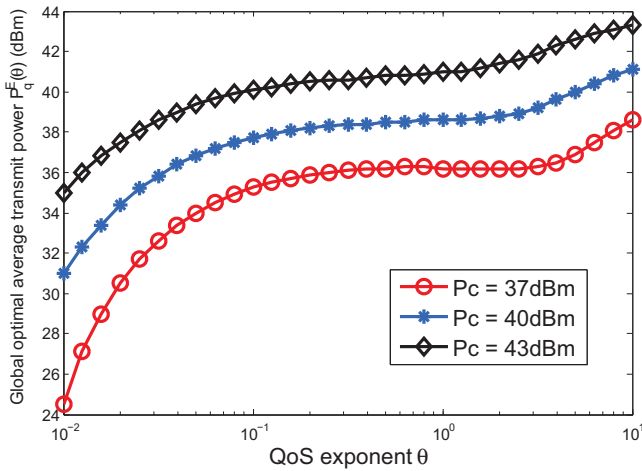


Fig. 7. The global optimal average transmit power under various QoS exponent.

efficiency is equal to 100%, 85%, 78.5%, 50%, and 25%, respectively. These settings of α are consistent with the average-transmit power-consumption coefficient of the popular power amplifiers such as Class-A, Class-B, and Class-D amplifiers as described in [28]. As illustrated in Fig. 5, the pentagram symbols denote the points of the global maximum ESE and the global maximum EPE corresponding to the specified α . The global maximum ESE and the global maximum EPE both decrease as α increases. This is because when α becomes larger, representing that the amplifier efficiency gets lower, the less power can be converted to transmit power, thus lowering the global maximum ESE and the global maximum EPE as compared to those with smaller α 's. The amplifiers with high amplifier efficiencies (i.e., small α 's) are usually employed for power saving, where α is close to 1. Thus, throughout the evaluations in Figs. 6-11, we set $\alpha = 1$.

Figures 6 and 7 depict the global maximum EPE and the global optimal average transmit power versus the QoS exponent, respectively. As shown in Fig. 6, the global maximum EPE decreases as the QoS exponent increases. This is because the increasing of average transmit power cannot compensate

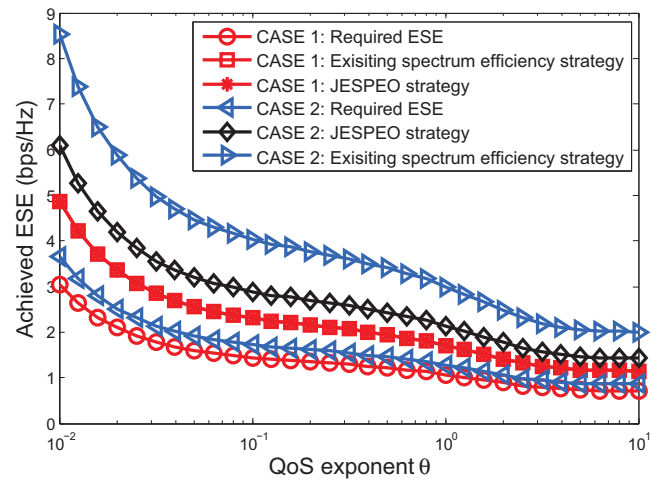


Fig. 8. The achieved ESE using the JESPEO strategy and the existing spectrum efficiency strategy.

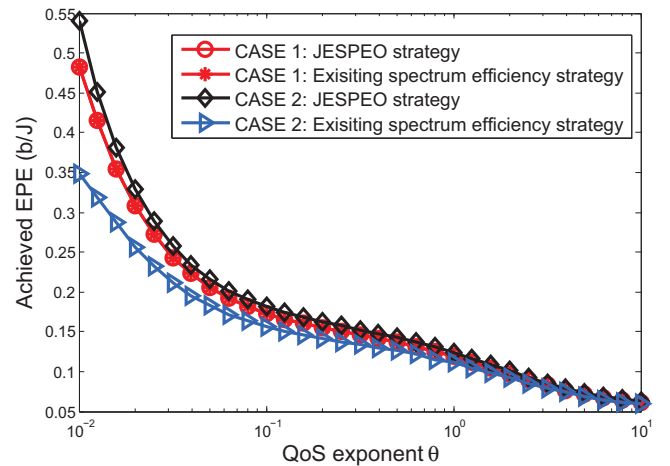


Fig. 9. The achieved EPE using the JESPEO strategy and the existing spectrum efficiency strategy.

for the EPE decreasing as the QoS exponent increases. As illustrated in Fig. 7, the global optimal average transmit power increases as the QoS exponent increases. This is because when the QoS exponent increases, the consumed average transmit power also needs to be increased to avoid the decrease of EPE. In Figs. 6 and 7, we set P_c to be 37 dBm (≈ 5 W), 40 dBm (10 W), and 43 dBm (≈ 20 W). These values represent the typical values of P_c for devices such as smart phones, tablets, and picocell/femtocell access points. We can observe that various values of circuit power allocation P_c do not impact the variation trends of the results (such as the global maximum EPE and $P_q^E(\theta)$).

Figures 8 and 9 plot the achieved ESE and the achieved EPE when using our proposed JESPEO strategy and the existing spectrum efficiency strategy [12] versus the QoS exponent, respectively. For CASE 1, we set the required and the maximum achievable ESEs as 50% and 80% of $C_q(\theta, P_q^E(\theta))$, respectively. For CASE 2, we set the required and the maximum achievable ESEs as 60% and 140% of $C_q(\theta, P_q^E(\theta))$, respectively. As shown in Fig. 9, our JESPEO strategy can get the same ESE as that of the existing spectrum

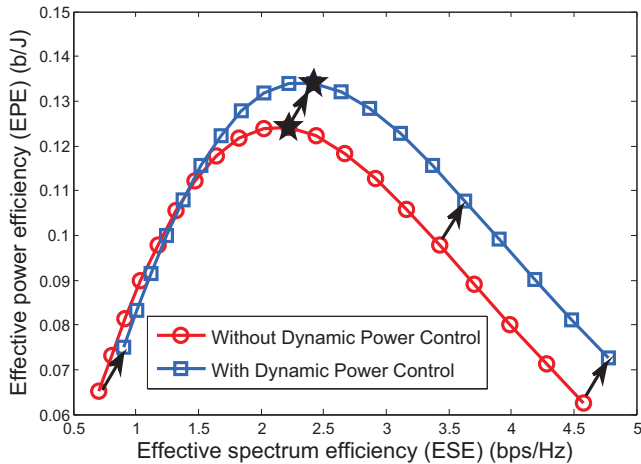


Fig. 10. The effective power efficiency versus the effective spectrum efficiency with and without the dynamic transmit power control ($\theta = 1$).

efficiency strategy for CASE 1 and can get larger ESE than the required ESE for CASE 2. As illustrated in Fig. 9, our JESPEO strategy can get the same EPE as that of the existing spectrum efficiency strategy for CASE 1 and can get larger EPE than that of the existing spectrum efficiency strategy for CASE 2. Because for both CASE 1 and CASE 2, our JESPEO strategy can get larger ESE than the required ESE and can obtain the maximum EPE simultaneously, and thus, the ESE and the EPE can be jointly optimized.

Figure 10 compares the EPE versus the ESE with and without the dynamic transmit power control when the QoS exponent is equal to 1. The average transmit power corresponding to the j -th circle symbol is equal to the average transmit power corresponding to the j -th square symbol (in Fig. 10, we have $1 \leq j \leq 20$). The pentagram symbols of both these two curves correspond to the global optimal average transmit power $P_q^E(\theta)$. From Fig. 10, we can observe that the effective spectrum and power efficiencies corresponding to the j -th circle symbol can be increased to the volume of the effective spectrum and power efficiencies corresponding to the j -th square symbol when we use the dynamic transmit power control. The effective spectrum and power efficiencies can be both increased not only in the MB region, but also in the CB region. Thus, the dynamic transmit power control strategy can jointly optimize the effective spectrum and power efficiencies without considering the region of the ESE. We can also observe that a small increase of the ESE can result in a large increase of the EPE.

Figure 11 evaluates the EPE versus the ESE using the MIMO-based strategy when the QoS exponent is equal to 1. The average transmit power corresponding to the k -th circle symbol, the k -th square symbol, and the k -th triangle symbol are the same (in Fig. 11, we have $1 \leq k \leq 12$). The pentagram symbols of these three curves correspond to the global optimal average transmit power $P_q^E(\theta)$. As illustrated in Fig. 11, the MIMO-based strategy can jointly optimize the effective spectrum and power efficiencies as compared with those of the single channel in SISO scheme. The effective spectrum and power efficiencies corresponding to the k -th circle symbol can be increased to the volume of

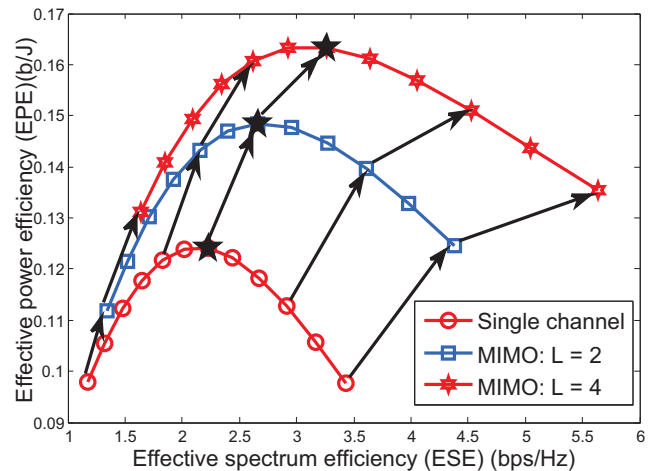


Fig. 11. The effective power efficiency versus the effective spectrum efficiency using the MIMO-based strategy ($\theta = 1$).

the effective spectrum and power efficiencies corresponding to the k -th square symbol when we use the $L = 2$ MIMO-based strategy instead of the single channel-based SISO scheme. The effective spectrum and power efficiencies corresponding to the k -th square symbol can be further increased to the volume of the effective spectrum and power efficiencies corresponding to the k -th triangle symbol when we use the $L = 4$ MIMO-based strategy instead of the $L = 2$ MIMO-based strategy. Moreover, the joint effective spectrum and power efficiencies optimization can be obtained not only in the MB region, but also in the CB region. Thus, without considering the region of the ESE, the MIMO-based strategy can jointly optimize the effective spectrum and power efficiencies as compared with those of the single channel-based SISO scheme.

VII. CONCLUSIONS

We proposed an efficient framework to jointly optimize spectrum and power efficiencies under different statistical delay-QoS guarantees for multimedia transmission over wireless fading channels in wireless networks. We identified the relationship between the effective spectrum efficiency and the effective power efficiency. Based on this relationship, we derived the mutual beneficial region and the contention-based region. We also analyzed the impact of statistical delay-QoS guarantees on the global maximum effective power efficiency and the global optimal average transmit power. In the mutual beneficial region, we developed the JESPEO strategy for joint effective spectrum and power efficiencies optimization. In the contention-based region, we developed the wireless-relay-based strategy to converge to the joint effective capacity and power efficiencies optimization. In both mutual beneficial and contention-based regions, we proposed the dynamic transmit power control strategy and the MIMO-based strategy for joint effective spectrum and power efficiencies optimization. Extensive numerical results verified our analyses of impact on statistical delay-QoS guarantees and showed that our strategies can significantly improve the joint spectrum and power efficiencies under diverse statistical delay-QoS guarantees in both mutual beneficial and contention-based regions.

APPENDIX A
PROOF OF LEMMA 2

Proof: We define $\bar{\mathbf{P}}(\theta) \triangleq (\bar{P}_1(\theta), \bar{P}_2(\theta), \dots, \bar{P}_L(\theta))$. Because the expectation operation in Eq. (36) is a linear operation, deriving the convexity of the objective function in Eq. (36) is equivalent to deriving the convexity of function $g(\bar{\mathbf{P}}(\theta)) = \prod_{\ell=1}^L (1 + \bar{P}_\ell(\theta)\gamma_\ell)^{-\beta}$ on the space spanned by $\bar{\mathbf{P}}(\theta)$.

To derive the convexity of $g(\bar{\mathbf{P}}(\theta))$ on the space spanned by $\bar{\mathbf{P}}(\theta)$, we need to obtain the sign of the Hessian of $g(\bar{\mathbf{P}}(\theta))$. The second-order derivatives and the second-order partial derivatives of $g(\bar{\mathbf{P}}(\theta))$ can be obtained as

$$\frac{\partial^2 g(\bar{\mathbf{P}}(\theta))}{\partial (\bar{P}_i(\theta))^2} = \frac{\beta(\beta+1)\gamma_i^2}{(1 + \bar{P}_i(\theta)\gamma_i)^2} \prod_{\ell=1}^L (1 + \bar{P}_\ell(\theta)\gamma_\ell)^{-\beta} \quad (40)$$

and

$$\frac{\partial^2 g(\bar{\mathbf{P}})}{\partial \bar{P}_i(\theta) \partial \bar{P}_j(\theta)} = \frac{\beta^2 \gamma_i \gamma_j}{(1 + \bar{P}_i(\theta)\gamma_i)(1 + \bar{P}_j(\theta)\gamma_j)} \cdot \prod_{\ell=1}^L (1 + \bar{P}_\ell(\theta)\gamma_\ell)^{-\beta}, \quad i \neq j, \quad (41)$$

where $1 \leq i, j \leq L$. Then, we can derive the Hessian of $g(\bar{\mathbf{P}})$, denoted by $G(g(\bar{\mathbf{P}}))$, as follows:

$$G(g(\bar{\mathbf{P}})) = \beta \prod_{\ell=1}^L (1 + \bar{P}_\ell(\theta)\gamma_\ell)^{-\beta} \left[\beta \mathbf{Y}^T \mathbf{Y} + \text{diag} \left(\frac{1}{(1 + \bar{P}_1(\theta)\gamma_1)^2}, \dots, \frac{1}{(1 + \bar{P}_L(\theta)\gamma_L)^2} \right) \right], \quad (42)$$

where

$$\mathbf{Y} = \left(\frac{1}{1 + \bar{P}_1(\theta)\gamma_1}, \frac{1}{1 + \bar{P}_2(\theta)\gamma_2}, \dots, \frac{1}{1 + \bar{P}_L(\theta)\gamma_L} \right) \quad (43)$$

is a non-zero vector. Thus, for any non-zero vector $\mathbf{u} = (u_1, u_2, \dots, u_L)$, we get

$$\mathbf{u} G(g(\bar{\mathbf{P}})) \mathbf{u}^T = \beta \prod_{\ell=1}^L (1 + \bar{P}_\ell(\theta)\gamma_\ell)^{-\beta} \left[\beta (\mathbf{u} \mathbf{Y}^T)^2 + \sum_{\ell=1}^L \left(\frac{u_\ell}{1 + \bar{P}_\ell(\theta)\gamma_\ell} \right)^2 \right] > 0. \quad (44)$$

Therefore, we get that $G(g(\bar{\mathbf{P}}))$ is positive definite and thus $g(\bar{\mathbf{P}})$ is strictly convex on the space spanned by $\bar{\mathbf{P}}(\theta)$. Therefore, Lemma 2 follows. ■

APPENDIX B
PROOF OF THEOREM 2

Proof: We formulate the Lagrangian for **P2**, denoted by $J(\bar{P}_\ell(\theta))$, as follows:

$$J(\bar{P}_\ell(\theta)) = \mathbb{E}_\gamma \left\{ \prod_{\ell=1}^L (1 + \bar{P}_\ell(\theta)\gamma_\ell)^{-\beta} \right\} + \lambda \left(\mathbb{E}_\gamma \left\{ \sum_{\ell=1}^L \bar{P}_\ell(\theta) \right\} - \mathbb{E}_\gamma \{ \bar{P}_t(\theta) \} \right) - \kappa \bar{P}_\ell(\theta), \quad (45)$$

where $\lambda \geq 0$ and $\kappa \geq 0$ are the Lagrangian multipliers associated with Eqs. (34) and (35), respectively. The optimal solution $\bar{P}_\ell^*(\theta)$ ($1 \leq \ell \leq L$) and the optimal Lagrangian multipliers of optimization problem **P2** satisfy the following KKT conditions [26]:

$$\begin{cases} \frac{\partial J(\bar{P}_\ell(\theta))}{\partial \bar{P}_\ell(\theta)} \Big|_{\bar{P}_\ell(\theta)=\bar{P}_\ell^*(\theta)} = 0, & 1 \leq \ell \leq L; \\ \lambda^* \geq 0; \\ \lambda^* \left(\mathbb{E}_\gamma \left\{ \sum_{\ell=1}^L \bar{P}_\ell^*(\theta) \right\} - \mathbb{E}_\gamma \{ \bar{P}_t(\theta) \} \right) = 0; \\ \kappa^* \geq 0; \\ \kappa^* \bar{P}_\ell(\theta) = 0. \end{cases} \quad (46)$$

where λ^* and κ^* are the optimal Lagrangian multipliers corresponding to Eqs. (34) and (35), respectively. Solving Eq. (46), we can obtain the optimal solution $\bar{P}_\ell^*(\theta)$ ($1 \leq \ell \leq L$) which is given by Eq. (38). ■

REFERENCES

- [1] J. N. Laneman, D. N. C. Tse, and G. W. Wornell, "Cooperative diversity in wireless networks: Efficient protocols and outage behavior," *IEEE Trans. Inf. Theory*, vol. 50, no. 12, pp. 3062–3080, Dec. 2004.
- [2] D. Soldani and S. Dixit, "Wireless relays for broadband access [radio communications series]," *IEEE Commun. Mag.*, vol. 46, no. 3, pp. 58–66, Mar. 2008.
- [3] G. J. Foschini, "Layered space time architecture for wireless communication in a fading environment when using multiple antennas," *Bell Labs Syst. Tech. J.*, vol. 1, pp. 41–59, Autumn 1996.
- [4] L. Zheng and D. N. C. Tse, "Diversity and multiplexing: a fundamental tradeoff in multiple-antenna channels," *IEEE Trans. Inf. Theory*, vol. 49, no. 5, pp. 1073–1096, May 2003.
- [5] FCC, "Et docket no. 03-237," http://hraunfoss.fcc.gov/edocs/_public/attachmatch/FCC-03-289A1.pdf, Nov. 2003.
- [6] S. Haykin, "Cognitive radio: Brain-empowered wireless communications," *IEEE J. Sel. Areas Commun.*, vol. 23, no. 2, pp. 201–220, Feb. 2005.
- [7] G. Miao, N. Himayat, and G. Y. Li, "Energy-efficient link adaptation in frequency-selective channels," *IEEE Trans. Commun.*, vol. 58, no. 2, pp. 545–554, Feb. 2010.
- [8] Y. Chen, S. Zhang, S. Xu, and G. Y. Li, "Fundamental trade-offs on green wireless networks," *IEEE Commun. Mag.*, vol. 49, no. 6, pp. 30–37, Feb. 2011.
- [9] W. Cheng, X. Zhang, H. Zhang, and Q. Wang, "On-demand based wireless resources trading for green communications," in *Proc. IEEE INFOCOM 2011 Workshop on Green Communications and Networking*, Shanghai, China, Mar. 2011, pp. 283–288.
- [10] B. Wang, Y. Wu, F. Han, Y. H. Yang, and K. J. R. Liu, "Green wireless communications: A time-reversal paradigm," *IEEE J. Sel. Areas Commun.*, vol. 29, no. 8, pp. 1698–1710, Sep. 2011.
- [11] A. J. Goldsmith and S.-G. Chua, "Variable-rate variable-power MQAM for fading channels," *IEEE Trans. Commun.*, vol. 45, no. 10, pp. 1218–1230, Oct. 1997.
- [12] A. J. Goldsmith, *Wireless Communications*, Cambridge University Press, 2005.
- [13] F. Meshkati, H. V. Poor, S. C. Schwartz, and R. V. Balan, "Energy-efficient resource allocation in wireless networks with quality-of-service constraints," *IEEE Trans. Commun.*, vol. 57, no. 11, pp. 3406–3414, Nov. 2009.
- [14] G. Miao, N. Himayat, G. Y. Li, and S. Talwar, "Low-complexity energy-efficient scheduling for uplink ofdma," *IEEE Trans. Commun.*, vol. 60, no. 1, pp. 112–120, Jan. 2012.
- [15] D. P. Wu and R. Negi, "Effective capacity: a wireless link model for support of quality of service," *IEEE Trans. Wireless Commun.*, vol. 2, no. 4, pp. 630–643, July 2003.
- [16] X. Zhang and Q. Du, "Cross-layer modeling for QoS-driven multimedia multicast/broadcast over fading channels in [advances in mobile multimedia]," *IEEE Commun. Mag.*, vol. 45, no. 8, pp. 62–70, Aug. 2007.
- [17] J. Tang and X. Zhang, "Quality-of-service driven power and rate adaptation over wireless links," *IEEE Trans. Wireless Commun.*, vol. 6, no. 8, pp. 3058–3068, Aug. 2007.

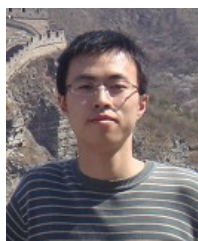
- [18] A. J. Fehske, F. Richter, and G. P. Fettweis, "Energy efficiency improvements through micro sites in cellular mobile radio networks," in *Proc. IEEE GLOBECOM Workshops*, Honolulu, Hawaii, Dec. 2009, pp. 1–5.
- [19] W. Cheng, H. Zhang, L. Zhao, and Y. Li, "Energy efficient spectrum allocation for green radio in two-tier cellular networks," in *Proc. IEEE GLOBECOM*, Miami, USA, Dec. 2010, pp. 1–5.
- [20] C. Khirallah, D. Vukobratovic, and J. Thompson, "On energy efficiency of joint transmission coordinated multi-point in LTE-advanced," in *Proc. International ITG Workshop on Smart Antennas (WSA)*, Dresden, Germany, Mar. 2012, pp. 54–61.
- [21] R. Irmer, H. Droste, P. Marsch, M. Grieger, G. Fettweis, S. Brueck, H.-P. Mayer, L. Thiele, and V. Jungnickel, "Coordinated multipoint: concepts, performance, and field trial results," *IEEE Commun. Mag.*, vol. 49, no. 2, pp. 102–111, Feb. 2011.
- [22] C. S. Chang, "Stability, queue length, and delay of deterministic and stochastic queueing networks," *IEEE Trans. Autom. Contr.*, vol. 39, no. 5, pp. 913–931, May 1994.
- [23] C. S. Chang, *Performance Guarantees in Communication Networks*, Springer-Verlag London, 2000.
- [24] M. A. Marsan, L. Chiaraviglio, D. Ciullo, and M. Meo, "Optimal energy savings in cellular access networks," in *Proc. IEEE ICC 2009 Workshops*, Dresden, Germany, June 2009, pp. 1–5.
- [25] Z. Niu, Y. Wu, J. Gong, and Z. Yang, "Cell zooming for cost-efficient green cellular networks," *IEEE Commun. Mag.*, vol. 48, no. 11, pp. 74–79, Nov. 2010.
- [26] S. Boyd and L. Vandenberghe, *Convex Optimization*, Cambridge University Press, 2004.
- [27] D. Tse and P. Viswanath, *Fundamentals of Wireless Communication*, Cambridge University Press, 2005.
- [28] Boylestad R. and L. Nashelsky, *Electronic Devices and Circuit Theory*, Prentice Hall College Division, 1996.



Xi Zhang (S'89-SM'98) received the B.S. and M.S. degrees from Xidian University, Xi'an, China, the M.S. degree from Lehigh University, Bethlehem, PA, all in electrical engineering and computer science, and the Ph.D. degree in electrical engineering and computer science (Electrical Engineering-Systems) from The University of Michigan, Ann Arbor.

He is currently an Associate Professor and the Founding Director of the Networking and Information Systems Laboratory, Department of Electrical and Computer Engineering, Texas A&M University, College Station. He was a research fellow with the School of Electrical Engineering, University of Technology, Sydney, Australia, and the Department of Electrical and Computer Engineering, James Cook University, Australia. He was with the Networks and Distributed Systems Research Department, AT&T Bell Laboratories, Murray Hill, New Jersey, and AT&T Laboratories Research, Florham Park, New Jersey, in 1997. He has published more than 250 research papers on wireless networks and communications systems, network protocol design and modeling, statistical communications, random signal processing, information theory, and control theory and systems. He received the U.S. National Science Foundation CAREER Award in 2004 for his research in the areas of mobile wireless and multicast networking and systems. He is an IEEE Distinguished Lecturer. He received Best Paper Awards at IEEE GLOBECOM 2007, IEEE GLOBECOM 2009, and IEEE WCNC 2010, respectively. He also received a TEES Select Young Faculty Award for Excellence in Research Performance from the Dwight Look College of Engineering at Texas A&M University, College Station, in 2006.

Prof. Zhang is serving or has served as an Editor for IEEE TRANSACTIONS ON COMMUNICATIONS, IEEE TRANSACTIONS ON WIRELESS COMMUNICATIONS, and IEEE TRANSACTIONS ON VEHICULAR TECHNOLOGY, twice as a Guest Editor for IEEE JOURNAL ON SELECTED AREAS IN COMMUNICATIONS for two special issues on "Broadband Wireless Communications for High Speed Vehicles" and "Wireless Video Transmissions," an Associate Editor for IEEE COMMUNICATIONS LETTERS, a Guest Editor for *IEEE Communications Magazine* and *IEEE Wireless Communications*, an Editor for Wiley's JOURNAL ON WIRELESS COMMUNICATIONS AND MOBILE COMPUTING, JOURNAL OF COMPUTER SYSTEMS, NETWORKING, AND COMMUNICATIONS, and Wiley's JOURNAL ON SECURITY AND COMMUNICATIONS NETWORKS, and an Area Editor for Elsevier's JOURNAL ON COMPUTER COMMUNICATIONS, among others. He is serving or has served as the TPC Chair for IEEE GLOBECOM 2011, TPC Vice-Chair IEEE INFOCOM 2010, TPC Area Chair for IEEE INFOCOM 2012, Panel/Demo/Poster Chair for ACM MobiCom 2011, General Vice-Chair for IEEE WCNC 2013, Panel/Demo/Poster Chair for ACM MobiCom 2011, and TPC/General Chair for numerous other IEEE/ACM conferences, symposia, and workshops.



Wencheng Cheng received B.S. degree in Telecommunication Engineering from Xidian University, Xi'an, China, in 2008. He is currently working towards a Ph.D. degree at Department of Telecommunication Engineering, Xidian University. He worked as a visiting Ph.D. student with Prof. Xi Zhang at Networking and Information Systems Laboratory, Department of Electrical and Computer Engineering, Texas A&M University, College Station, Texas, U.S.A., from 2010 to 2011, under the joint Ph.D. program between Department of Electrical and Computer

Engineering, Texas A&M University and Department of Telecommunication Engineering, Xidian University.

His research interests focus on wireless full-duplex transmission, statistical QoS provisioning, cognitive radio techniques, and energy efficient wireless networks. He has published multiple papers in IEEE INFOCOM, IEEE GLOBECOM, IEEE ICC, etc.



Hailin Zhang (M'98) received B.S. and M.S. degrees from Northwestern Polytechnic University, Xi'an, China, in 1985 and 1988 respectively, and the Ph.D. from Xidian University, Xi'an, China, in 1991. In 1991, he joined School of Telecommunications Engineering, Xidian University, where he is a senior Professor and the Dean of this school. He is also currently the Director of Key Laboratory in Wireless Communications Sponsored by China Ministry of Information Technology, a key member of State Key Laboratory of Integrated Services Networks,

one of the state government specially compensated scientists and engineers, a field leader in Telecommunications and Information Systems in Xidian University, an Associate Director for National 111 Project. Dr. Zhang's current research interests include key transmission technologies and standards on broadband wireless communications for B3G, 4G, and next generation broadband wireless access systems. He has published more than 100 papers in journals and conferences.